Scientific Journal of King Faisal University:
Basic and Applied Sciences

Assessing Drought Patterns Using Landsat-Derived Vegetation Health Index During Spring (2013–2024)

Almustafa Abd Elkader Ayek [1], Suzan Fathe Karmoka [2], Abdullah Taher Hasan [3] and Mohannad Ali Loho [4,5]

[1] Department of Topography, Faculty of Civil Engineering, University of Aleppo, Aleppo, 12212, Syria
[2] Department of Agricultural Studies and Research, General Organization of Remote Sensing (GORS), Damascus, Syria
[3] Department of Geography, Faculty of Arts and Humanities, University of Aleppo, Aleppo, 12212, Syria
[4] Department of Geography, Faculty of Arts and Humanities, Tartous University, Tartous, Syria
[5] Department of Geography, Faculty of Arts and Humanities, Damascus University, Damascus, Syria

LINK	RECEIVED	ACCEPTED	PUBLISHED ONLINE	ASSIGNED TO AN ISSUE
https://doi.org/10.37575/b/agr/250013	17/03/2025	21/05/2025	21/05/2025	01/06/2025
NO. OF WORDS	**NO. OF PAGES**	**YEAR**	**VOLUME**	**ISSUE**
5674	6	2025	26	1

ABSTRACT

This study aims to assess drought patterns in the Harem region of northwestern Syria during the spring seasons from 2013 to 2024, using data from Landsat 8 and 9. Drought severity was evaluated and categorized into five classes using the Vegetation Health Index, which combines the Normalized Difference Vegetation Index and the Temperature Condition Index. Monthly precipitation data were included as a supporting component to evaluate climatic conditions, and the Google Earth Engine platform was used for processing and spatiotemporal analysis. The findings revealed fluctuations in drought severity, with the 2017–2019 period being the most affected, particularly in 2019, when land surface temperature (LST) reached its highest levels and vegetation health markedly declined. The 2020–2024 period, by contrast, showed gradual improvement in vegetation health and a reduction in the extent of severe drought. The study also indicated that the relationship between precipitation and drought severity is nonlinear, with LST playing a key role in determining drought intensity. To improve the management of water and agricultural resources and reduce the effects of drought on local communities and ecosystems, this study highlights the importance of adopting advanced monitoring and forecasting strategies that incorporate artificial intelligence technology.

KEYWORDS

Abiotic stress, climate change, dissertation, prediction, water resources, weather forecast

CITATION

Ayek, A.A.E., Karmoka, S.F. Hasan, A.T. and Loho, M.A. (2025). Assessing drought patterns using landsat-derived vegetation health index during spring (2013–2024). *Scientific Journal of King Faisal University: Basic and Applied Sciences*, **26**(1), 51–6. DOI: 10.37575/b/agr/250013

1. Introduction

One of the most hazardous natural occurrences that has a significant impact on ecosystems and human communities worldwide is drought. Tracking and evaluating the impacts of drought is more challenging because, unlike other natural catastrophes that strike quickly, it develops slowly and has lingering effects that can last for months or even years (Sugg *et al.*, 2020; Wilhite and Glantz, 1985). Global climate change has worsened the issue in recent decades by increasing the frequency and severity of drought occurrences (Trenberth *et al.*, 2014). This growing threat highlights the urgent need to develop advanced and efficient tools and techniques for drought monitoring and impact analysis on both the environment and communities (Kim and Jehanzaib, 2020; Adisa, Masinde, and Botai, 2020). Syria is also frequently exposed to drought. Over the past few decades, the country has witnessed an increase in the frequency and severity of drought periods, which has exacerbated the problems of desertification and the degradation of agricultural lands. This has been reflected in living conditions and a decline in per capita income due to annual fluctuations in agricultural land productivity (Atik *et al.*, 2024). Several studies indicate that Syria has experienced multiple severe drought waves in recent decades (Karmoka *et al.*, 2019; Mathbout *et al.*, 2025), which has greatly affected water and agricultural resources (Hameed *et al.*, 2020). In this context, remote sensing technologies have played a vital role in enhancing our capacity for extensive drought monitoring (Kogan, 1995; Nepsta *et al.*, 1994). Recent years have witnessed tremendous advancements in these technologies, opening new avenues for real-time environmental change monitoring and analysis. The Landsat series of satellites stands out as one of the primary sources of space data among the crucial space tools contributing to drought studies, providing precise historical records spanning more than 40 years of continuous Earth surface observation (Belward and Skøien, 2015; Goward *et al.*, 2021; Wulder *et al.*, 2022). Landsat 8 and Landsat 9 satellites are capable of providing multispectral data at high spatial resolutions of up to 30 meters per pixel, with coverage cycles repeating every 16 days (Irons and Masek, 2006; Masek *et al.*, 2020; Roy *et al.*, 2014). These features make Landsat an ideal tool for monitoring changes in vegetation cover and land surface conditions, which helps improve our ability to track the effects of drought on the environment. The ability to analyze temporal and spatial changes using these space data provides valuable tools for researchers and planners to assess drought severity and predict potential impacts, enhancing adaptation strategies and reducing negative effects on local communities and ecosystems (Bhaga *et al.*, 2020; Zhang *et al.*, 2021). Recent studies show that remote sensing techniques can provide a thorough and precise representation of drought conditions, assisting in identifying vulnerable regions and assessing their severity (Agarwal *et al.*, 2024). Additional studies have demonstrated the value of these techniques in tracking variations in vegetation cover and understanding how drought impacts various ecosystems (Li *et al.*, 2024). With the increasing volume of available space data, there is a need for powerful platforms that can efficiently process and analyze these data. Google Earth Engine (GEE) represents a paradigm shift in this field, offering massive computing power and a vast archive of space data. The platform enables researchers and specialists to process and analyze large datasets without the need for extensive local computing resources and supports the development of interactive applications that can be shared with the scientific community (Ayek and Zerouali, 2025; Bhowmik and Bhatt, 2024; Qazvini and Carrion, 2023). The Vegetation Health Index (VHI) is an enhanced drought monitoring index (Hu *et al.*, 2020), which combines vegetation cover and land surface temperature (LST) information into a single index. The VHI integrates two main indices: the Vegetation Condition Index (VCI), based on the Normalized Difference Vegetation Index (NDVI), and the Temperature Condition

Corresponding Author: Almustafa Abd Elkader Ayek 009630959262134, almustafaayek@gmail.com

Index (TCI), based on LST, and measures plant heat stress. VHI has been applied in various environments and geographical areas. It can precisely identify agricultural drought conditions, detect early vegetation stress, and be used for studying various natural and cultivated vegetation covers (Alqadhi *et al.*, 2025; Hang *et al.*, 2024; Javan *et al.*, 2025; Karmoka and Hanjagi, 2023; Zeng *et al.*, 2022) to assess the impacts, severity, and classification of drought and to monitor the temporal and spatial changes of drought conditions. It may also be used to track actual vegetation drought across different agricultural and climatic regions while accounting for meteorological variables (Bhuiyan *et al.*, 2006). Given the increasing challenges of drought and its impacts on food security and water resources, there is an urgent need to develop user-friendly and effective drought monitoring applications. These applications can support decision-makers in water and agricultural resource management, researchers in studying drought patterns and trends, farmers in planning agricultural activities, and institutions in emergency planning and drought response. The present study aims to develop an integrated application on the GEE platform to derive and analyze the VHI using Landsat 8 and 9 data. The application focuses on areas with vegetation cover only to ensure assessment accuracy, provides an interactive user interface to select the analysis time period, calculates and analyzes drought intensity, and generates detailed reports on drought conditions. This study represents an important step toward developing effective drought monitoring tools that can be used by a wide range of users, contributing to improving our understanding and management of this complex natural phenomenon.

2. Materials and Methods

2.1. Study Area:

The Harem region is located in the northern part of the Idlib Governorate, in the far northwest of Syria. It extends between latitudes 35°55′50″ and 36°20′26″ north of the equator and longitudes 36°22′35″ and 36°49′59″ east of the Greenwich line (Figure 1). With an estimated area of 768 km², it constitutes 14.1% of the Idlib Governorate's total area. The Orontes (al-Asi) River forms its western boundary; Mount Simeon, its eastern boundary; the Amq Plain and the Afrin River, its northern boundary; and the Al-Roj Plain, its southern boundary.

Figure 1: The geographical location of the study area

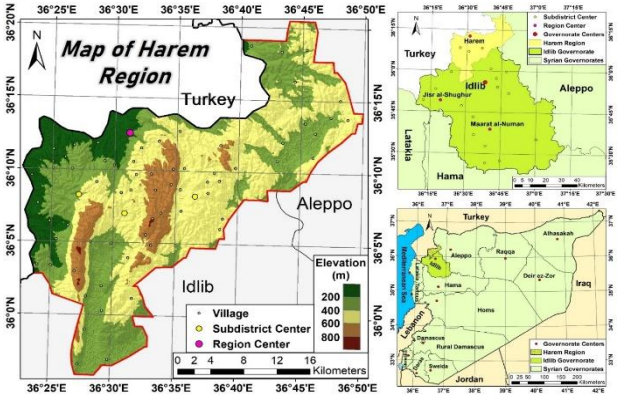

The region contains three low-lying hilly bands (Barisha, Al-A'la, Al-Wustani) that run along the north–south axis. The highest peak of Al-Wustani Mountain is 870 meters, while the lowest point is 89 meters, located north of Salqin near the Al-Omq depression. Plains and depressions such as Al-Roj, Sardin, and Al-Dana are also present and are hydrologically linked to the basin. The lower Orontes has a semi-humid Mediterranean climate with cold, rainy winters and moderate, dry summers.

2.2. Used Data:

An integrated set of satellite data from the Landsat 8 and Landsat 9 satellites was used. Together, they provide continuous coverage of Earth's surface every eight days at a spatial resolution of 30 meters. The Landsat Collection 2 Level-2 dataset was utilized, featuring advanced radiometric and geometric processing to ensure data quality and reliability. The data included the primary spectral bands for calculating the NDVI—the red band (SR_B4) and the near-infrared band (SR_B5)—as well as LST data derived from the thermal band (ST_B10) using the single channel algorithm. Additionally, monthly precipitation data from ERA5-Land were used to represent climatic conditions in the study area. The study period covered 2013 to 2024, focusing on the spring season (March to May), which represents the main vegetation growth period in the region.

2.3. Research Methodology:

The VHI was calculated and analyzed using a sequential system of related procedures (Figure 2). The process began with the preprocessing of raw data from Landsat 8 and 9. Quality masks were applied to exclude pixels affected by clouds and shadows. Spectral band values were converted to reflectance values, and thermal band data were converted to LSTs in Celsius. The red and near-infrared bands were used to calculate NDVI, and areas with vegetation cover were identified by excluding non-vegetated areas using an NDVI ≥ 0.2 threshold (Yu *et al.*, 2014).

Figure 2: Flow chart of research methodology

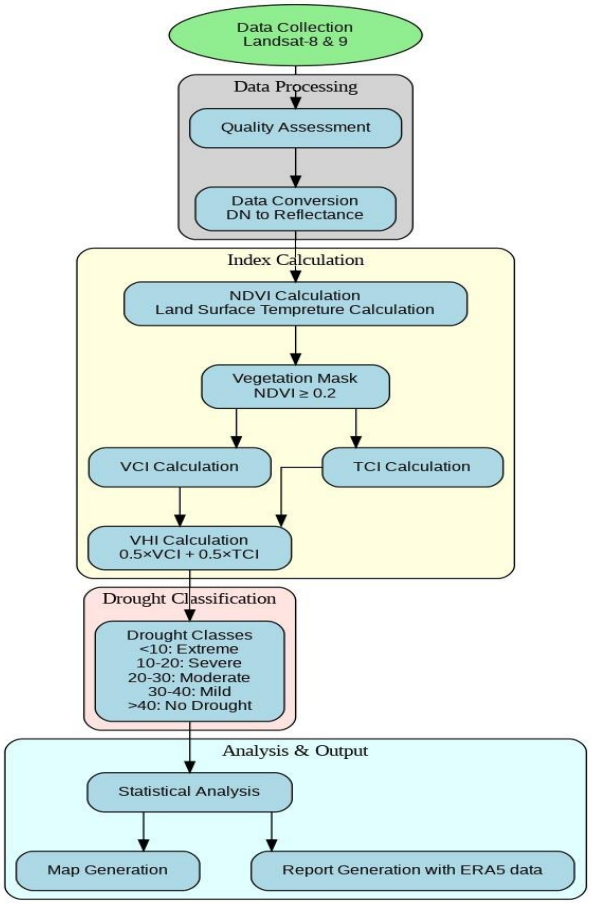

The NDVI was calculated using Equation (1) (Rouse *et al.*, 1973):

$$NDVI = \frac{NIR - RED}{NIR + RED} \quad (1)$$

Where *NIR* represents the near-infrared band surface reflectance, and *RED* represents the red band surface reflectance.

The VCI is calculated by determining the maximum ($NDVI_{max}$) and minimum ($NDVI_{min}$) values of the NDVI index for the study period by applying Equation (2) (Kogan, 1995).

$$VCI = \frac{NDVI - NDVI_{min}}{NDVI_{max} - NDVI_{min}} \times 100 \quad (2)$$

Concurrently, the TCI is calculated by applying Equation (3) (Kogan, 1995), using the maximum (LST_{max}) and minimum (LST_{min}) values of LST.

$$TCI = \frac{LST_{max} - LST_i}{LST_{max} - LST_{min}} \times 100 \quad (3)$$

Surface temperature values were extracted from Landsat Level 2 products using band ST_B10 by applying conversion factors (scale factor 0.00341802 and offset factor 149). The values were then converted from Kelvin to Celsius by subtracting 273.15 degrees (Equation 4) (USGS, 2023).

$$LST = [(ST\_B10 * 0.00431802) + 149] - 273.15 \quad (4)$$

The VCI and TCI indices are then combined with equal weights (0.5) to obtain the VHI, following Equation (5) (Kogan, 1995).

$$VHI = 0.5 \times VCI + 0.5 \times TCI \quad (5)$$

A diminished VHI value, resulting from a low NDVI and high LST, indicates suboptimal vegetative condition. In contrast, a higher VHI value, reflecting high NDVI and lower LST, suggests enhanced vegetation vitality and health (Tang *et al.*, 2020). The VHI is classified into five categories to determine drought severity: very severe drought (VHI < 10), severe drought (10–20), moderate drought (20–30), mild drought (30–40), and no drought (VHI ≥ 40).

The methodology concludes with a comprehensive statistical analysis, including calculation of the areas affected by each drought category and analysis of temporal and spatial changes. The results are presented as distribution maps and detailed statistical reports, supported by rainfall data to illustrate the relationship between drought and prevailing climatic conditions. The application, **Drought Watch**, is designed to display the VHI layer for each user analysis, showing a color gradient ranging from dark red (dry areas) to green (wet areas), within a numerical range of 0 to 50.

3. Results and Discussion

3.1. Temporal Analysis of Dry Periods:

With the exception of 2013, 2020, and 2024—when the area of the no-drought class constituted more than 50% of the study area, the results showed variation in the distribution of drought classes across the years, exceeding 50% in most years. In 2013 and 2020, the area of the no-drought category reached 570.42 km² and 527.11 km², respectively (Figure 3), reflecting the region's sensitivity to multiple climatic factors, most notably changes in precipitation amounts, LST, and human–economic impacts related to the war.

Figure 3: Drought severity trends over the years.

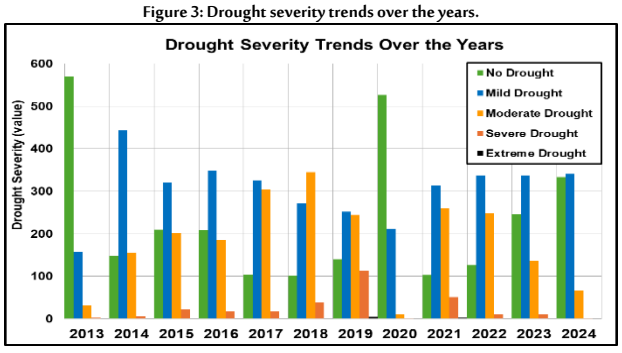

Three major phases can be distinguished within the study period:

3.1.1. Moderate to mild drought phase (2013–2016)

The extreme drought class was rare during this phase, with the area impacted by this class never exceeding 0.56 km² in any year. The percentage of regions not affected by drought (no-drought class) remained relatively high, reaching 570.42 km² in 2013 and decreasing to 208.29 km² in 2016 (Figure 3). The NDVI average fluctuated over this phase, with values ranging from 0.29 to 0.45 (Figure 5). Despite some stressful periods, the overall vegetation condition was considered good, with an index average of 0.38. During this phase, the average temperature was 31.58°C, and the average precipitation was 89.72 mm. The majority of the study area in 2013 appeared green, indicating high values of the VHI and, consequently, a vital vegetation cover and larger vegetated area. This is evident from the maps in Figure 4, which illustrate the temporal and spatial distribution of drought according to the VHI index. Although at a smaller percentage, the remaining years of this phase also displayed a spread of green (high VHI values).

Figure 4: The spatiotemporal distribution of VHI values during each phase

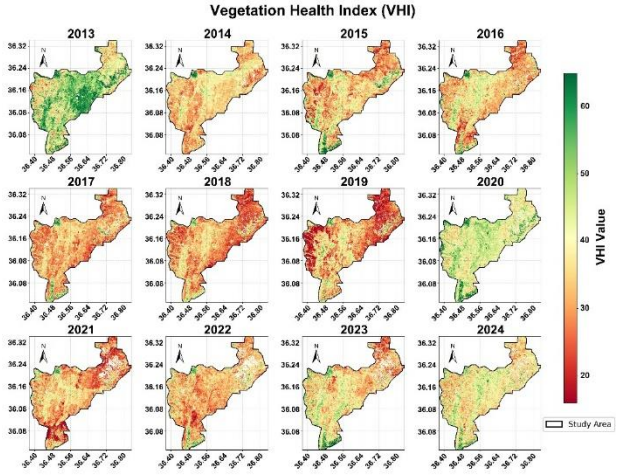

Figure 5: Standard deviation and average NDVI values for the studied time series

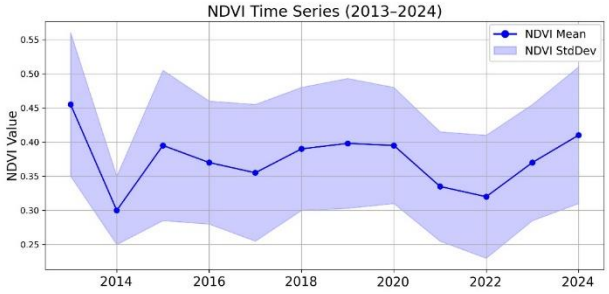

3.1.2. Severe drought phase (2016–2019)

The percentage of regions experiencing severe drought increased significantly during this phase, indicating that the vegetative cover was in an unhealthy condition with decreasing vitality. This is in line with the conclusion drawn by Mathbout *et al.* (2025), which showed that throughout the years 2008, 2010, 2016, and 2017, Syria witnessed a concentration of severe drought waves, especially in the central and northern regions. The phase was accompanied by an increase in the average LST, which recorded 32.1°C, indicating that temperature played a role in the drought condition during this period. Furthermore, it was accompanied by a notable increase in the average amount of precipitation (143.7 mm), suggesting that one of the primary causes of the drought's increased severity was the temperature rise. The highest percentage of areas experiencing severe drought in the time series,

113.54 km², was recorded in 2019. Numerous factors contributed to this, including natural ones such as high LSTs. For example, 2019 had the highest average surface temperature value during the study period at 34.9°C, indicating that the area experienced unusually high-water pressure in the spring of that year. Unnatural factors also played a role, including human activity through logging and overgrazing, particularly in areas with natural vegetation cover (FAO, 2020), as well as the consequences of the war, which affected the energy sector (fuel and electricity) required to supply irrigation water in agricultural areas (Jaafar *et al.*, 2017). This resulted in a decrease in the area of planted vegetation cover and a decline in its health and production status (Sukkar *et al.*, 2024). Based on the drought class distribution maps (Figure 4), the majority of areas appeared dark red, indicating a decline in the health and vitality of vegetation cover. This condition was due to heat stress from high LSTs and the accompanying human factors from military operations and the difficulty of accessing and maintaining agricultural lands. This indicates the state of severe drought during these years.

3.1.3. Gradual recovery phase (2020–2024)

During this phase, the areas afflicted by severe drought declined to only 1.75 km² in 2024, indicating a gradual enhancement in drought conditions and relative stability. On the other hand, the areas not impacted by drought expanded to 333.4 km² in 2024, showing that environmental conditions had generally improved. In addition, the average LST decreased to 28.56°C in 2024, reducing heat stress on plants, while the average precipitation was 114 mm during this phase. The year 2024 recorded a high rainfall of 124 mm. An obvious enhancement in vegetation cover was shown by the 2024 NDVI, which recorded one of the highest values in the time series at 0.41. Increased positive human activity and an effective precipitation–temperature balance contributed to this improvement. Due to better economic and environmental conditions, along with increased recent precipitation, the vegetation cover area (NDVI > 0.2) also expanded during this phase (Figure 6). In 2024, it increased to 741.39 km², indicating a gradual recovery of agricultural lands. Additionally, a decline in dark red–dominated regions was observed, reflecting the decrease in severe drought classes and the increase in areas showing no drought, indicated by green color shades. These areas were distributed throughout the study area (Figure 4), particularly in 2020, which witnessed a significant and rapid recovery of vegetation cover after the severe stress experienced in 2019. This recovery was attributed to the noticeable decline in average LST values by 2.95°C compared to 2019 and the accompanying improvement in precipitation, which reached 120.41 mm in 2020.

Figure 6: The vegetated cover area for the studied time series.

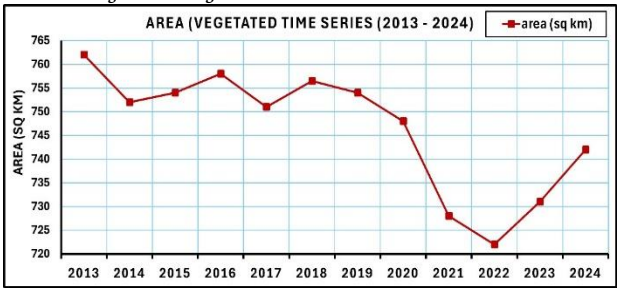

3.2. Factors that Influence Drought:

3.2.1. The relationship between surface temperatures and drought

- The findings demonstrated that high LSTs were frequently associated with severe droughts. For instance, despite relatively significant precipitation, 2019 witnessed a notable decline in vegetation health due to comparatively high temperatures.
- On the other hand, 2024 saw a temperature decrease compared to previous years, which had a positive impact on vegetation cover.

3.2.2. The role of precipitation

- Although precipitation plays a crucial role in determining the severity of drought, the results indicated that the relationship is not necessarily linear. The mean NDVI values and rainfall amounts showed a weak and insignificant correlation (R = 0.09).
- In some years, such as 2019, high precipitation did not have a clear positive effect on reducing drought due to high temperatures and their negative effects on soil and vegetation.
- In contrast, in other years, such as 2023 and 2024, precipitation played a more prominent role in improving environmental conditions, as reflected in the general enhancement of vegetation health indicators and the high value of actual precipitation in these two years.

4. Conclusions

This study assessed drought patterns and vegetation health in the Harem region from 2013 to 2024, and the main findings are summarized as follows:

- Since 2019 experienced the greatest rate of severe drought and the highest LSTs during the research period, it can be considered the peak drought year.
- In recent years (2020–2024), the study area has gradually improved, with an increase in the area of healthy vegetation and a decrease in drought intensity.
- The relationship between precipitation and drought severity is not direct, as LSTs play a crucial role in determining the extent to which vegetation is affected by drought. Therefore, the prevalence and severity of drought cannot be judged based on rainfall alone; temperature levels must also be considered. This makes monitoring climate change essential for understanding drought dynamics.
- In the long term, the results revealed a persistent pattern of mild drought in the region, with affected areas ranging between 200 and 400 km² during most of the study years. It was noted that very severe drought events, although relatively rare, remained intermittently present, indicating that the region experiences frequent cycles of stress due to high temperatures or human-induced destruction of agricultural lands and a decline in agricultural service operations.
- The results also showed significant variation in the distribution of different drought classes between years, with 2017 having a large area impacted by moderate drought (304.07 km²), while 2018 recorded the largest area of moderate drought (344.5 km²).
- Regarding vegetation cover, the area covered by vegetation progressively shrank (NDVI ≥ 0.2) from 760.97 km² in 2013 to the lowest value of 723.08 km² in 2022.

5. Recommendations

- The study area, Harem, is located within Idlib Governorate, which borders Turkey. Since the outbreak of the Syrian crisis, this area has witnessed ongoing military operations and widespread population displacement. During the study period (2013–2024), the area was outside the scope of any government support, regulation, or monitoring programs, resulting in a complete absence of data on the vegetation inventory or the state of the region's ecosystems. Furthermore, no reports were available from any governmental or non-governmental entity documenting the state of the vegetation cover during this period.
- This demonstrates the practical significance of the model, as it provides real-time and rapid data on the current state of vegetation cover and drought conditions in the region. It highlights the importance of the model and its potential to assist decision-makers in proposing necessary measures as quickly as possible after detecting an environmental problem. The model relies on the GEE platform, which provides continuous data with a long archive and near-real-time updates. It also helps decision-makers identify and navigate to affected areas to carry out rapid intervention and support operations, serving as a spatial indicator that accurately identifies areas exposed to climatic and non-climatic stresses. The model is distinguished by its potential for application in other areas, expanding its usefulness in supporting environmental and agricultural rehabilitation efforts.
- The study area urgently needs rehabilitation of existing irrigation networks and the establishment of new ones to meet agricultural development needs. Depending on the availability of groundwater resources, it is also suggested to establish a network of wells to enhance available water sources.
- To achieve resource sustainability and improve agricultural

productivity, it is recommended to implement modern irrigation projects aimed at minimizing water waste and optimizing water use. It is also suggested to expand the use of drought-resistant agricultural varieties in line with prevailing climatic conditions.

- To support farmers and enable them to replant their lands, it is essential to provide improved seeds, fertilizers, and other agricultural production inputs. Additionally, a structured pastoral program should be established to determine the appropriate seasons for opening and closing pastures, thus protecting vegetation cover while ensuring fodder needs are met.
- Based on these results, along with time series analysis approaches to forecast future developments, it is crucial to improve ongoing monitoring of LST, as it is closely associated with drought changes. Since NDVI, LST, and precipitation data can be integrated to produce more precise studies of long-term drought trends, creating AI-based models (neural networks and deep learning) is a promising first step in this direction. This will help empower decision-makers to take proactive steps to safeguard agricultural resources and reduce the detrimental effects of drought on regional ecosystems.
- Furthermore, the use and analysis of thermal sensor data in parallel with soil and moisture information can be a key component in improving the accuracy of drought assessment.
- This approach opens new avenues for understanding the impacts of drought on agricultural production and vegetation cover, helping to develop more efficient strategies to mitigate its effects and enhance the sustainability of ecosystems and agriculture in the future.

Data Availability Statement

The data that support the findings of this study are available on request from the corresponding author.

Acknowledgments

The authors extend their appreciation for the continued support of University of Aleppo, General Organization of Remote Sensing, Tartous University and Damascus University.

Funding

This research received no external funding.

Conflicts of Interest

No conflicts of interest exist.

Biographies

Almustafa AbdElkader Ayek

Department of Civil Engineering, Faculty of Civil Engineering, University of Aleppo, Aleppo, Syria, 009630959262134, almustafaayek@gmail.com

Ayek, a Syrian researcher with a Civil Engineering (Topography) degree from the University of Aleppo, specializes in remote sensing and GIS. His work focuses on water resource monitoring, land surface temperature retrieval, and spatial analysis. He publishes in peer-reviewed journals and develops applications using Google Earth Engine. Ayek also delivers GIS and remote sensing training, engaging both academics and professionals through his practical expertise and research contributions.

ORCID: 0009-0007-5952-8239

Suzan Fathe Karmoka

Department of Agricultural Research, Center for Remote Sensing Studies and Research, General Organization of Remote Sensing (GORS), Damascus, Syria, 0096399287360, karmoka.suzan@hotmail.com

Suzan is a Ph.D. scholar in Remote Sensing and Environment at Bangalore University. She holds an MSc in Renewable Natural Resources and Environment from Damascus University, Syria. She is a research assistant at GORS and formerly served as a research engineer at GCSAR. Suzan has taught remote sensing at Damascus University, Bangalore University, and NIE Mysore. She has published widely, participated in conferences, and contributed to RS/GIS training programs locally and with international organizations like the FAO.

ORCID: 0000-0003-4567-305X

Abdullah Taher Hasan

Department of Geography, Faculty of Arts and Humanities, University of Aleppo in Liberated Areas, Aleppo, Syria, 00963969154710, abdullahtaherhasan@gmail.com

Abdullah is a Syrian researcher specializing in GIS and remote sensing, with a Master's degree from the University of Aleppo in Liberated Areas. His research focuses on applying these technologies to rainwater harvesting and groundwater exploration in Syria. He is particularly interested in geo-AI for groundwater detection and karst geomorphology. Abdullah lectures part-time at the University of Aleppo, teaching climate, environment, and social geography, and is currently preparing to present his Ph.D. research proposal.

ORCID: 0009-0001-3902-1189

Mohannad Ali Loho

Department of Geography, Faculty of Arts and Humanities, Tartous University, Tartous, Syria, 00963988268102, mohannad.loho@damascusuniversity.edu.sy, mohannad609@gmail.com

Mohannad is a Syrian researcher specializing in GIS, remote sensing, and spatial AI applications. He holds a master's degree in Geography from the University of Damascus, with a focus on GIS. He has authored Syrian geography textbooks and developed hundreds of maps. As a lecturer at Tartus University, he teaches GIS, cartography, surveying, and land use. Currently pursuing a Ph.D., his research focuses on AI-driven land use monitoring and prediction. He has published and submitted several peer-reviewed studies.

ORCID: 0009-0002-5024-9798

References

Adisa, O.M., Masinde, M., Botai, J.O. and Botai, C.M. (2020). Bibliometric analysis of methods and tools for drought monitoring and prediction in Africa. *Sustainability,* **12**(16), 6516. DOI: 10.3390/su12166516.

Agarwal, V., Singh, B.V.R., Marsh, S., Qin, Z., Sen, A. and Kulhari, K. (2025). Integrated remote sensing for enhanced drought assessment: A multi‐index approach in Rajasthan, India. *Earth and Space Science,* **12**(2), e2024EA003639. DOI: 10.1029/2024EA003639.

Alqadhi, S., Mallick, J. and Hang, H.T. (2025). Assessing drought trends and vegetation health in arid regions using advanced remote sensing techniques: A case study in Saudi Arabia. *Theoretical and Applied Climatology,* **156**(1), 1–29. DOI: 10.1007/s00704-024-05301-1.

Atik, O., Kadour, A., Mahmoud, I., Al Hasan, K., Al Nabhan, A., Jazieh, H., Nijhawan, A. and Pianosi, F. (2024). Irrigation water in Northwest Syria: Impact of the recent crisis and drought. *Water,* **16**(21), 3101. DOI: 10.3390/w16213101.

Ayek, A.A. and Zerouali, B. (2025). Monitoring temporal changes of the Qttinah Lake surface area using Landsat data and Google Earth Engine. *DYSONA–Applied Science,* **6**(1), 126–33. DOI: 10.30493/das.2024.476854.

Belward, A.S. and Skøien, J.O. (2015). Who launched what, when and why: Trends in global land-cover observation capacity from civilian Earth observation satellites. *ISPRS Journal of Photogrammetry and Remote Sensing,* **103**(n/a), 115–28. DOI: 10.1016/j.isprsjprs.2014.03.009.

Bhaga, T.D., Dube, T., Shekede, M.D. and Shoko, C. (2020). Impacts of climate variability and drought on surface water resources in Sub-Saharan Africa using remote sensing: A review. *Remote Sensing,* **12**(24), 4184. DOI: 10.3390/rs12244184.

Bhowmik, S. and Bhatt, B. (2024). Drought monitoring using MODIS-derived indices and Google Earth Engine platform for Vadodara District, Gujarat. *Journal of the Indian Society of Remote Sensing,* **52**(9), 1885–900. DOI: 10.1007/s12524-024-01922-1.

Bhuiyan, C., Singh, R.P. and Kogan, F.N. (2006). Monitoring drought dynamics in the Aravalli region (India) using different indices based on ground and remote sensing data. *International Journal of Applied Earth Observation and Geoinformation,* **8**(4), 289–302. DOI: 10.1016/j.jag.2006.03.002.

Food and Agriculture Organization (FAO). (2020). *Evaluation of FAO's contribution to the Syrian Arab Republic 2012–2018* (Country Programme Evaluation Series, 12/2020). Rome. Available at: https://openknowledge.fao.org/handle/20.500.14283/cb2475en (accessed on 17/04/2025)

Ghaleb, F., Mario, M. and Sandra, A.N. (2015). Regional Landsat-based drought monitoring from 1982 to 2014. *Climate,* **3**(3), 563–77. DOI: 10.3390/cli3030563.

Goward, S.N., Masek, J.G., Loveland, T.R., Dwyer, J.L., Williams, D.L., Arvidson, T., Rocchio, L.E.P. and Irons, J.R. (2021). Semi-centennial of Landsat observations and Pending Landsat 9 launch. *Photogrammetric Engineering and Remote Sensing,* **87**(8), 533–9. DOI: 10.14358/PERS.87.8.533.

Hameed, M., Ahmadalipour, A. and Moradkhani, H. (2020). Drought and food security in the Middle East: An analytical framework. *Agricultural and Forest Meteorology,* **281**(n/a), 107816. DOI: 10.1016/j.agrformet.2019.107816.

Hang, Q., Guo, H., Meng, X., Wang, W., Cao, Y., Liu, R., De Maeyer, P. and Wang, Y. (2024). Optimizing the Vegetation Health Index for agricultural drought monitoring: Evaluation and application in the Yellow River Basin. *Remote Sensing,* **16**(23), 4507. DOI: 10.3390/rs16234507.

Hu, T., van Dijk, A.I.J.M., Renzullo, L.J., Xu, Z., He, J., Tian, S., Zhou, J. and Li, H. (2020). On agricultural drought monitoring in Australia using Himawari-8 geostationary thermal infrared observations. *International Journal of Applied Earth Observation and Geoinformation,* **91**(n/a), 102153. DOI: 10.1016/j.jag.2020.102153.

Irons, J.R. and Masek, J.G. (2006). Requirements for a Landsat data continuity mission. *Photogrammetric Engineering and Remote Sensing,* **72**(10), 1102.

Jaafar, H.H., Zurayk, R., King, C., Ahmad, F. and Al-Outa, R. (2017). Impact of the Syrian conflict on irrigated agriculture in the Orontes Basin. In: *The water-energy-food nexus in the Middle East and North Africa*, Routledge. DOI: 10.1080/07900627.2015.1023892.

Javan, F.D., Samadzadegan, F., Toosi, A. and TousiKordkolaei, H. (2025). Spatial-temporal patterns of agricultural drought severity in the Lake Urmia Basin, Iran: A cloud-based integration of multi-temporal and multi-sensor remote sensing data. *DYSONA–Applied Science,* **6**(2), 239–61. DOI: 10.30493/DAS.2025.486806.

Karmoka, S.F. and Hanjagi, D.A. (2023). Detecting the vegetation health situation of Tartus forests (Syria) and the spatio-temporal distribution of agricultural drought. In: *International Scientific Conference of Young Scientists and Specialists Dedicated to the 180th Anniversary of the Birth of K.A. Timiryazev: Collection of Articles,* **2**(n/a), 527–32. 05–07/06/2023 DOI: 10.5281/zenodo.13693241.

Karmoka, S.F., Al haj Ahmad, A. and Alkhaled, E.A. (2019). Identifying drought classes in Northwest Syria using MODIS satellite image spectral indices EVI, LAI, TVI'. *Scientific Journal of King Faisal University: Basic and Applied Sciences,* **20**(1), 27–39.

Kim, T.W. and Jehanzaib, M. (2020). Drought risk analysis, forecasting and assessment under climate change. *Water,* **12**(7), 1862. DOI: 10.3390/w12071862.

Kogan, F.N. (1995). Application of vegetation index and brightness temperature for drought detection. *Advances in Space Research,* **15**(11), 91–100. DOI: 10.1016/0273-1177(95)00079-T.

Li, T. and Zhong, S. (2024). Advances in optical and thermal remote sensing of vegetative drought and phenology. *Remote Sensing,* **16**(22), 4209. DOI: 10.3390/rs16224209.

Masek, J.G., Wulder, M.A., Markham, B., McCorkel, J., Crawford, C.J., Storey, J. and Jenstrom, D.T. (2020). Landsat 9: Empowering open science and applications through continuity. *Remote Sensing of Environment,* **248**(n/a), 111968. DOI: 10.1016/j.rse.2020.111968.

Masitoh, F. and Rusydi, A.N. (2019). Vegetation Health Index (VHI) analysis during drought season in Brantas Watershed. In: *IOP Conference Series: Earth and Environmental Science* **389**(1), 012033. IOP Publishing. DOI: 10.1088/1755-1315/389/1/012033.

Mathbout, S., Boustras, G., Papazoglou, P., Vide, J.M. and Raai, F. (2025). Integrating climate indices and land use practices for comprehensive drought monitoring in Syria: Impacts and implications. *Environmental and Sustainability Indicators*, **26**(n/a), 100631. DOI: 10.1016/j.indic.2025.100631.

Nepstad, D.C., de Carvalho, C.R., Davidson, E.A., Jipp, P.H., Lefebvre, P.A., Negreiros, G.H. and Vieira, S. (1994). The role of deep roots in the hydrological and carbon cycles of Amazonian forests and pastures. *Nature,* **372**(6507), 666–9. DOI: 10.1038/372666a0.

Rouse Jr, J.W., Haas, R.H., Schell, J.A. and Deering, D.W. (1973). *Monitoring the vernal advancement and retrogradation (green wave effect) of natural vegetation* (No. NASA-CR-132982). Available at: https://ntrs.nasa.gov/citations/19750020419 (accessed on 01/05/2025).

Roy, D.P., Wulder, M.A., Loveland, T.R., Woodcock, C.E., Allen, R.G., Anderson, M.C. and Zhu, Z. (2014). Landsat-8: Science and product vision for terrestrial global change research. *Remote Sensing of Environment,* **145**(n/a), 154–72. DOI: 10.1016/j.rse.2014.02.001.

Sugg, M., Runkle, J., Leeper, R., Bagli, H., Golden, A., Handwerger, L.H. and Woolard, S. (2020). A scoping review of drought impacts on health and society in North America. *Climatic Change,* **162**(n/a), 1177–95. DOI: 10.1007/s10584-020-02848-6.

Sukkar, A., Abulibdeh, A., Essoussi, S. and Seker, D.Z. (2024). Investigating the impacts of climate variations and armed conflict on drought and vegetation cover in Northeast Syria (2000–2023). *Journal of Arid Environments,* **225**(n/a), 105278. DOI: 10.1016/j.jaridenv.2024.105278.

Taheri Qazvini, A. and Carrion, D. (2023). A spatiotemporal drought analysis application implemented in the Google Earth Engine and applied to Iran as a case study. *Remote Sensing,* **15**(9), 2218. DOI: 10.3390/rs15092218.

Tang, J., Zeng, J., Zhang, Q., Zhang, R., Leng, S., Zeng, Y. and Wang, Q. (2020). Self-adapting extraction of cropland phenological transitions of rotation agroecosystems using dynamically fused NDVI images. *International Journal of Biometeorology,* **64**(n/a), 1273–83. DOI: 10.1007/s00484-020-01904-1.

Trenberth, K.E., Dai, A., Van der Schrier, G., Jones, P.D., Barichivich, J., Briffa, K.R. and Sheffield, J. (2014). Global warming and changes in drought. *Nature Climate Change,* **4**(1), 17–22. DOI: 10.1038/nclimate2067.

U.S. Geological Survey. (2023). *Landsat 8–9 Collection 2 Level 2 Science Product Guide* (Version 5.0). U.S. Department of the Interior. Available at: https://www.usgs.gov (accessed on 07/02/2025)

Wilhite, D.A. and Glantz, M.H. (1985). Understanding the drought phenomenon: The role of definitions. *Water International,* **10**(3), 111–20. DOI: 10.1080/02508068508686328.

Wulder, M.A., Roy, D.P., Radeloff, V.C., Loveland, T.R., Anderson, M.C., Johnson, D.M. and Cook, B.D. (2022). Fifty years of Landsat science and impacts. *Remote Sensing of Environment,* **280**(n/a), 113195. DOI: 10.1016/j.rse.2022.113195.

Zeng, J., Zhang, R., Qu, Y., Bento, V.A., Zhou, T., Lin, Y. and Wang, Q. (2022). Improving the drought monitoring capability of VHI at the global scale via ensemble indices for various vegetation types from 2001 to 2018. *Weather and Climate Extremes,* **35**(n/a), 100412. DOI: 10.1016/j.wace.2022.100412.

Zhang, Z., Xu, W., Shi, Z. and Qin, Q. (2021). Establishment of a comprehensive drought monitoring index based on multisource remote sensing data and agricultural drought monitoring. *IEEE Journal of Selected Topics in Applied Earth Observations and Remote Sensing,* **14**(n/a), 2113–26. DOI: 10.1109/JSTARS.2021.3052194.

Yu, X., Guo, X. and Wu, Z. (2014). Land surface temperature retrieval from Landsat 8 TIRS—Comparison between radiative transfer equation-based method, split window algorithm and single channel method. *Remote Sensing,* **6**(10), 9829–52. DOI: 10.3390/rs6109829.